Fizika Nizkikh Temperatur, 2004, v. 30, Nos. 7/8, p. 814–822

Fractional ac Josephson effect in unconventional superconductors

Hyok-Jon Kwon[1], K. Sengupta[2], and Victor M. Yakovenko[1]

[1]*Department of Physics, University of Maryland, College Park, Maryland 20742-4111, USA*

[2]*Department of Physics, Yale University, New Haven, Connecticut 06520-8120, USA*
E-mail: yakovenk@physics.umd.edu

Received January 5, 2004

For certain orientations of Josephson junctions between two p_x-wave or two d-wave superconductors, the subgap Andreev bound states produce a 4π-periodic relation between the Josephson current I and the phase difference φ: $I \propto \sin(\varphi/2)$. Consequently, the ac Josephson current has the fractional frequency $eV/\hbar$, where V is the dc voltage. In the tunneling limit, the Josephson current is proportional to the first power (not square) of the electron tunneling amplitude. Thus, the Josephson current between unconventional superconductors is carried by single electrons, rather than by Cooper pairs. The fractional ac Josephson effect can be observed experimentally by measuring frequency spectrum of microwave radiation from the junction.

PACS: **74.50.+r,** 74.70.Kn, **74.72.–h**

1. Brief history of the ac Josephson effect

In 1962, Josephson [1] predicted theoretically that if a dc voltage V is applied to a junction between two superconductors, ac supercurrent with the frequency $2eV/\hbar$ appears between the superconductors. The ac Josephson radiation was first observed experimentally 40 years ago in Kharkov by Yanson, Svistunov, and Dmitrenko [2,3]. In Ref. 3, the spectrum of microwave radiation from tin junctions was measured and a sharp peak in the frequency spectrum at $2eV/\hbar$ was found. It is amazing that without any attempt to match impedances of the junction and waveguide, Dmitrenko and Yanson [3] found the signal several hundred times stronger than the noise and the ratio of linewidth to the Josephson frequency less than 10^{-3}. This discovery was followed by further work in the United States [4] and Ukraine [5]. The results of these investigations were summarized in the classic book [6]. Since then, the ac Josephson radiation has been observed in many materials in various experimental setups. For example, a peak of Josephson radiation was found in Ref. 7 in indium junctions at the frequency 9 GHz with the width 36 MHz. In Ref. 8, a peak of Josephson radiation was observed around 11 GHz with the width 50 MHz in $Bi_2Sr_2CaCu_2O_8$ single crystals with the current along the **c** axis perpendicular to the layers.

The theory of the Josephson effect was originally developed for conventional s-wave superconductors. In this paper, we study Josephson junctions between unconventional superconductors, such as d-wave cuprates or p_x-wave organic superconductors. We show that the midgap Andreev states in these materials produce a 4π-periodic relation between the Josephson current I and the phase difference φ: $I \propto \sin(\varphi/2)$. Consequently, the ac Josephson current has the fractional frequency $eV/\hbar$, a half of the conventional value. We hope that this effect can be observed experimentally as the corresponding peak in the frequency spectrum of Josephson radiation from unconventional superconductors, such as d-wave cuprates, in the manner similar to the pioneering experiments [2,3] performed on conventional s-wave superconductors.

2. Introduction

In many materials, the symmetry of the superconducting order parameter is unconventional, i.e., not s-wave. In the high-T_c cuprates, it is the singlet $d_{x^2-y^2}$-wave [9]. There is experimental evidence that, in the quasi-one-dimensional (Q1D) organic superconductors $(TMTSF)_2X$ [10], the symmetry is triplet [11], most likely the p_x-wave [12], where the x axis is along the conducting chains. The unconventional pair-

ing symmetry typically results in formation of midgap Andreev bound states on the surfaces of these superconductors. For *d*-wave cuprate superconductors, the midgap Andreev states were predicted theoretically in Ref. 13 and discovered experimentally as a zero-bias conductance peak in tunneling between normal metals and superconductors (see Ref. 14). For the Q1D organic superconductors, the midgap states were theoretically predicted to exist at the edges perpendicular to the chains [15,16]. When two unconventional superconductors are joined together in a Josephson junction, their Andreev surface states hybridize to form Andreev bound states in the junction. These states are important for the Josephson current. Andreev bound states in high-T_c junctions were reviewed in Ref. 17. The Josephson effect between two Q1D *p*-wave superconductors was studied in Refs. 18 and 19.

In the present paper, we predict a new effect for Josephson junctions between unconventional (nonchiral) superconductors, which we call the fractional ac Josephson effect. Suppose both superconductors forming a Josephson junction have surface midgap states originally. This is the case for the butt-to-butt junction between two p_x-wave Q1D superconductors, as shown in Fig. 1,*a*, and for the 45°/45° in-plane junction between two *d*-wave superconductors, as shown in Fig. 3,*a*. (The two angles indicate the orientation of the junction line relatively to the **b** axes of each $d_{x^2-y^2}$ superconductor.) We predict that the contribution of the hybridized Andreev bound states produces a 4π-periodic relation between the supercurrent I and the superconducting phase difference φ: $I \propto \sin(\varphi/2)$ [20]. Consequently, the ac Josephson effect has the frequency $eV/\hbar$, where e is the electron charge, V is the applied dc voltage, and h is the Planck constant. The predicted frequency is a half of the conventional Josephson frequency $2eV/\hbar$ originating from the conventional Josephson relation $I \propto \sin\varphi$ with the period of 2π. Qualitatively, the predicted effect can be understood as follows. The Josephson current across the two unconventional superconductors is carried by tunneling of single electrons (rather than Cooper pairs) between the two resonant midgap states. Thus, the Cooper pair charge $2e$ is replaced by the single charge e in the expression for the Josephson frequency. This interpretation is also supported by the finding that, in the tunneling limit, the Josephson current is proportional to the first power (not square) of the electron tunneling amplitude [21–23]. Possibilities for experimental observation of the fractional ac Josephson effect are discussed in Sec. 4.

The predicted current-phase relation $I \propto \sin(\varphi/2)$ is quite radical, because every textbook on superconductivity says that the Josephson current must be a 2π-periodic function of φ [20]. To our knowledge, the only paper that discussed the 4π-periodic Josephson effect is Ref. 24 by Kitaev. He considered a highly idealized model of spinless fermions on a one-dimensional (1D) lattice with superconducting pairing on the neighboring sites. The pairing potential in this case has the p_x-wave symmetry, and midgap states do exist at the ends of the chain. They are described by the Majorana fermions, which Kitaev proposed to use for nonvolatile memory in quantum computing. He found that, when two such superconductors are brought in contact, the system is 4π-periodic in the phase difference between the superconductors. Our results are in agreement with his work. However, we formulate the problem as an experimentally realistic Josephson effect between known superconducting materials.

3. The basics

In this paper, we consider singlet pairing and triplet pairing with the spin polarization vector **n** having a uniform, momentum-independent orientation [11,12]. If the spin quantization axis z is selected along **n**, then the Cooper pairing takes a place between electrons with the opposite z axis spin projections σ and $\bar{\sigma}$: $\left\langle \hat{c}_\sigma(\mathbf{k})\hat{c}_{\bar{\sigma}}(-\mathbf{k})\right\rangle \propto \Delta_\sigma(\mathbf{k})$, where $\hat{c}_\sigma(\mathbf{k})$ is the annihilation operator of an electron with momentum **k** and spin σ. The pairing potential has the symmetry $\Delta_\sigma(\mathbf{k}) = \mp\Delta_{\bar{\sigma}}(\mathbf{k}) = \pm\Delta_\sigma(-\mathbf{k})$, where the upper and lower signs correspond to the singlet and triplet cases.

We select the coordinate axis x perpendicular to the Josephson junction plane. We assume that the interface between the two superconductors is smooth enough, so that the electron momentum component k_y parallel to the junction plane is a conserved good quantum number.

Electron states in a superconductor are described by the Bogoliubov operators $\hat{\gamma}$, which are related to the electron operators $\hat{c}$ by the following equations [25]

$$\hat{\gamma}_{n\sigma k_y} = \int dx[u^*_{n\sigma k_y}(x)\hat{c}_{\sigma k_y}(x) + v^*_{n\sigma k_y}(x)\,\hat{c}^\dagger_{\bar{\sigma}\bar{k}_y}(x)], \tag{1}$$

$$\hat{c}_{\sigma k_y}(x) = \sum_n [u_{n\sigma k_y}(x)\hat{\gamma}_{n\sigma k_y} + v^*_{n\bar{\sigma}\bar{k}_y}(x)\hat{\gamma}^\dagger_{n\bar{\sigma}\bar{k}_y}], \tag{2}$$

where $\bar{k}_y = -k_y$, and n is the quantum number of the Bogoliubov eigenstates. The two-components vectors $\psi_{n\sigma k_y}(x) = [u_{n\sigma k_y}(x), v_{n\sigma k_y}(x)]$ are the eigenstates of the Bogoliubov–de Gennes (BdG) equation with the eigenenergies $E_{n\sigma k_y}$:

$$\begin{pmatrix} \varepsilon_{k_y}(\hat{k}_x) + U(x) & \hat{\Delta}_{\sigma k_y}(x,\hat{k}_x) \\ \Delta^\dagger_{\sigma k_y}(x,\hat{k}_x) & -\varepsilon_{k_y}(\hat{k}_x) - U(x) \end{pmatrix} \psi_n = E_n\psi_n, \tag{3}$$

where $\hat{k}_x = -i\partial_x$ is the x component of the electron momentum operator, and $U(x)$ is a potential. In Eq. (3) and below, we often omit the indices σ and k_y to shorten notation where it does not cause confusion.

4. Junctions between quasi-one-dimensional superconductors

In this Section, we consider junctions between two Q1D superconductors, such as organic superconductors $(TMTSF)_2X$, with the chains along the x axis, as shown in Fig. 1,*a*. For a Q1D conductor, the electron energy dispersion in Eq. (3) can be written as $\varepsilon = \hbar^2 k_x^2/2m - 2t_b \cos(bk_y) - \mu$, where m is an effective mass, μ is the chemical potential, b and t_b are the distance and the tunneling amplitude between the chains. The superconducting pairing potentials in the s- and p_x-wave cases have the forms

$$\hat{\Delta}_{\sigma k_y}(x, \hat{k}_x) = \begin{cases} \sigma\Delta_\beta, & s\text{-wave}, \\ \Delta_\beta \hat{k}_x/k_F, & p_x\text{-wave}, \end{cases} \qquad (4)$$

where $\hbar k_F = \sqrt{2m\mu}$ is the Fermi momentum, and σ is treated as + for $\uparrow$ and − for $\downarrow$. The index $\beta = R, L$ labels the right ($x > 0$) and left ($x < 0$) sides of the junction, and Δ_β acquires a phase difference φ across the junction:

$$\Delta_L = \Delta_0, \qquad \Delta_R = \Delta_0 e^{i\varphi}. \qquad (5)$$

The potential $U(x) = U_0\delta(x)$ in Eq. (3) represents the junction barrier located at $x = 0$. Integrating Eq. (3) over x from -0 to $+0$, we find the boundary conditions at $x = 0$:

$$\psi_L = \psi_R, \qquad \partial_x\psi_R - \partial_x\psi_L = k_F Z\psi(0), \qquad (6)$$

$$Z = 2mU_0/\hbar^2 k_F, \qquad D = 4/(Z^2 + 4), \qquad (7)$$

where D is the transmission coefficient of the barrier.

4.1. Andreev bound states

A general solution of Eq. (3) is a superposition of the terms with the momenta close to αk_F, where the index $\alpha = \pm$ labels the right- and left-moving electrons:

$$\psi_{\beta\sigma} = e^{\beta\kappa x}\left[A_\beta \begin{pmatrix} u_{\beta\sigma+} \\ v_{\beta\sigma+} \end{pmatrix} e^{i\tilde{k}_F x} + B_\beta \begin{pmatrix} u_{\beta\sigma-} \\ v_{\beta\sigma-} \end{pmatrix} e^{-i\tilde{k}_F x}\right]. \qquad (8)$$

Here $\beta = \mp$ for R and L. Eq. (8) describes a subgap bound state with an energy $|E| < \Delta_0$, which is localized at the junction and decays exponentially in x within the length $1/\kappa$. The coefficients $(u_{\beta\sigma\alpha}, v_{\beta\sigma\alpha})$ in Eq. (8) are determined by substituting the right- and left-moving terms separately into Eq. (3) for $x \neq 0$, where $U(x) = 0$. In the limit $k_F >> \kappa$, we find

$$\frac{u_{\beta\sigma\alpha}}{v_{\beta\sigma\alpha}} = \frac{\Delta_{\beta\sigma\alpha}}{E + i\alpha\beta\hbar\kappa v_F}, \qquad \kappa = \frac{\sqrt{\Delta_0^2 - |E|^2}}{\hbar v_F}, \qquad (9)$$

where $v_F = \hbar k_F/m$ is the Fermi velocity, and $\Delta_{\beta\sigma\alpha}$ is equal to $\sigma\Delta_\beta$ for s-wave and to $\alpha\Delta_\beta$ for p_x-wave, with Δ_β given by Eq. (5). The k_y-dependent Fermi momentum $\hbar\tilde{k}_F = \hbar k_F + 2t_b \cos(bk_y)/v_F$ in Eq. (8) eliminates the dispersion in k_y from the BdG equation.

Substituting Eq. (8) into the boundary conditions (6), we obtain the linear homogeneous equations for the coefficients A_β and B_β. The compatibility condition for these equations gives an equation for the energies of the Andreev bound states. There are two subgap states with the energies $E_a = aE_0(\varphi)$ labeled by the index $a = \pm$:

$$E_0^{(s)}(\varphi) = -\Delta_0\sqrt{1 - D\sin^2(\varphi/2)}, \quad s\text{–}s \text{ junction}, \qquad (10)$$

$$E_0^{(p)}(\varphi) = -\Delta_0\sqrt{D}\cos(\varphi/2), \quad p_x\text{–}p_x \text{ junction}. \qquad (11)$$

The energies (10) and (11) are plotted as functions of φ in the left panels (*b*) and (*c*) of Fig. 1. Without barrier ($D = 1$), the spectra of the $s-s$ and p_x-p_x junctions are the same and consist of two crossing curves $E = \mp\Delta_0\cos(\varphi/2)$, shown by the thin lines in the left panel of Fig. 1,*b*. A non-zero barrier ($D < 1$) changes the energies of the Andreev bound states in the $s-s$ and p_x-p_x junctions in different ways. In the $s-s$ case, the two energy levels repel near $\varphi = \pi$ and form two separated 2π-periodic branches shown by the thick lines in the left panel of Fig. 1,*b* [25,26]. In contrast, in the p_x-p_x case, the two energy levels continue to cross at $\varphi = \pi$, and they are separated from the continuum of states above $+\Delta_0$ and below $-\Delta_0$, as shown in the left panel of Fig. 1,*c*. The absence of energy levels repulsion indicates that there is no matrix element between these levels at $\varphi = \pi$ in the p_x-p_x case, unlike in the $s-s$ case.

As shown in Sec. 5, the 45°/45° junction between two d-wave superconductors is mathematically equivalent to the p_x-p_x junction. Eq. (11) was derived for the 45°/45° junction in Ref. 22,23, and 27.

4.2. dc Josephson effect in thermodynamic equilibrium

It is well known [25,28] that the current carried by a quasiparticle state a is

$$I_a = \frac{2e}{\hbar}\frac{\partial E_a}{\partial\varphi}. \qquad (12)$$

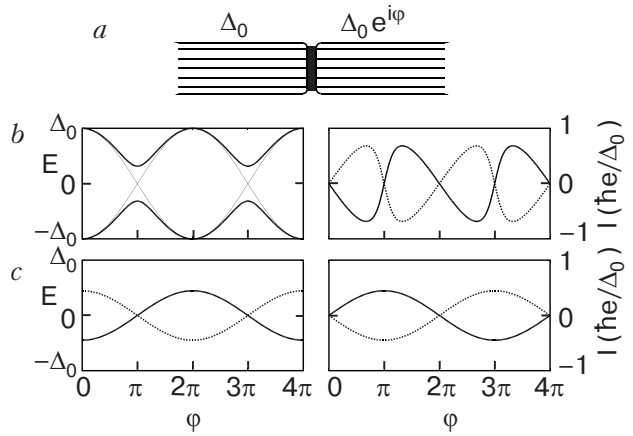

Fig. 1. Josephson junction between two Q1D p_x-wave superconductors (*a*). The energies (left panel) and the currents (right panel) of the subgap states in the $s-s$ junction as functions of the phase difference φ for $D = 1$ (thin lines) and $D = 0.9$ (thick lines) (*b*). The same as (*b*) for the p_x-p_x junction at $D = 0.2$ (*c*).

The two subgap states carry opposite currents, which are plotted versus φ in the right panels (*b*) and (*c*) of Fig. 1 for the $s-s$ and p_x-p_x junctions. In thermodynamic equilibrium, the total current is determined by the Fermi occupation numbers f_a of the states at temperature T:

$$I = \frac{2e}{\hbar}\sum_{a=\pm}\frac{\partial E_a}{\partial\varphi}f_a = -\frac{2e}{\hbar}\frac{\partial E_0}{\partial\varphi}\tanh\left(\frac{E_0}{2T}\right). \quad (13)$$

For the $s-s$ junction, substituting Eq. (10) into Eq. (13), we recover the Ambegaokar–Baratoff formula [29] in the tunneling limit $D << 1$.

$$I_s \approx D\sin\varphi\,\frac{e\Delta_0}{2\hbar}\tanh\left(\frac{\Delta_0}{2T}\right) = \sin\varphi\,\frac{\pi\Delta_0}{2eR}\tanh\left(\frac{\Delta_0}{2T}\right) \quad (14)$$

and the Kulik–Omelyanchuk formula [30] in the transparent limit $D \to 1$

$$I_s \approx \sin\left(\frac{\varphi}{2}\right)\frac{e\Delta_0}{\hbar}\tanh\left(\frac{\Delta_0\cos(\varphi/2)}{2T}\right). \quad (15)$$

Taking into account that the total current is proportional to the number N of conducting channels in the junction (e.g., the number of chains), we have replaced the transmission coefficient D in Eq. (14) by the junction resistance $R = \hbar/2Ne^2D$ in the normal state.

Substituting Eq. (11) into Eq. (13), we find the Josephson current in p_x-p_x junction in thermodynamic equilibrium:

$$I_p = \sqrt{D}\sin\left(\frac{\varphi}{2}\right)\frac{e\Delta_0}{\hbar}\tanh\left(\frac{\Delta_0\sqrt{D}\cos(\varphi/2)}{2T}\right) =$$

$$= \sin\left(\frac{\varphi}{2}\right)\frac{\pi\Delta_0}{\sqrt{D}eR}\tanh\left(\frac{\Delta_0\sqrt{D}\cos(\varphi/2)}{2T}\right). \quad (16)$$

The temperature dependences of the critical currents for the $s-s$ and p_x-p_x junctions are shown in Fig. 2. They are obtained from Eqs. (14) and (16) assuming the BCS temperature dependence for Δ_0. In the vicinity of T_c, I_p, and I_s have the same behavior. With the decrease of temperature, I_s quickly saturates to a constant value, because, for $D << 1$, $E_a^{(s)} \approx \mp\Delta_0$ (10), thus, for $T \lesssim \Delta_0$, the upper subgap state is empty and the lower one is completely filled. In contrast, I_p rapidly increases with decreasing temperature as $1/T$ and saturates to a value enhanced by the factor $2/\sqrt{D}$ relative to the Ambegaokar–Baratoff formula (10) at $T = 0$. This is a consequence of two effects. As Eqs. (14) and (16) show, $I_s \propto D$ and $I_p \propto \sqrt{D}$, thus $I_p >> I_s$ in the tunneling limit $D << 1$. At the same time, the energy splitting between the two subgap states in the p_x-p_x junction is small compared to the gap: $E_0^{(p)} \propto \sqrt{D}\Delta_0 << \Delta_0$. Thus, for $\sqrt{D}\Delta_0 \lesssim T \lesssim \Delta_0$, the two subgap states are almost equally populated, so the critical current has the $1/T$ temperature dependence analogous to the Curie spin susceptibility.

Equation (16) was derived analytically for the 45°/45° junction between two *d*-wave superconductors in Refs. 21,22, and a similar result was calculated numerically for the p_x-p_x junction in Refs. 18,19. Notice that Eq. (16) gives the Josephson current $I_p(\varphi)$ that is a 2π-periodic functions of φ, both for $T = 0$ and $T \neq 0$. This is a consequence of the thermo-

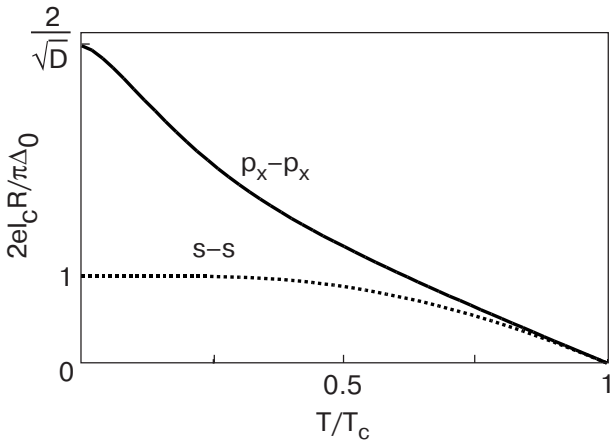

Fig. 2. Critical current of the $s-s$ (dashed line) and p_x-p_x (solid line) Josephson junction as function of temperature for $D = 0.3$.

dynamic equilibrium assumption. At $T = 0$, this assumption implies that the subgap state with the lower energy is occupied, and the one with the higher energy is empty. As one can see in Fig. 1, the lower energy is always a 2π-periodic functions of φ. The assumption of thermodynamic equilibrium was explicitly made in Ref. 22 and was implicitly invoked in Refs. 18,19, and 21 by using the Matsubara diagram technique. In Ref. 31, temperature dependence of the Josephson critical current was measured in the YBCO ramp–edge junctions with different crystal angles and was found to be qualitatively consistent with the upper curve in Fig. 2.

4.3. Dynamical fractional ac Josephson

The calculations of the previous section are applied in the static case, where a given phase difference φ is maintained for an infinitely long time, so the occupation numbers of the subgap states have enough time to relax to thermodynamic equilibrium. Now let us consider the opposite dynamical limit. Suppose a small voltage $eV << \Delta_0$ is applied to the junction, so the phase difference acquires dependence on time t: $\varphi(t) = 2eVt/\hbar$. In this case, the state of the system is determined dynamically starting from the initial conditions. Let us consider the $p_x - p_x$ junction at $T = 0$ in the initial state $\varphi = 0$, where the two subgap states (11) with the energies $\pm E_0$ are, correspondingly, occupied and empty. If $\varphi(t)$ changes sufficiently slowly (adiabatically), the occupation numbers of the subgap states do not change. In other words, the states shown by the solid and dotted lines in Fig. 1,*c* remains, correspondingly, occupied and empty. The occupied state (11) produces the current (12):

$$I_p(t) = \frac{\sqrt{D}e\Delta_0}{\hbar}\sin\left(\frac{\varphi(t)}{2}\right) = \frac{\sqrt{D}e\Delta_0}{\hbar}\sin\left(\frac{eVt}{\hbar}\right). \quad (17)$$

The frequency of the ac current (17) is $eV/\hbar$, a half of the conventional Josephson frequency $2eV/\hbar$. The fractional frequency can be traced to the fact that the energies of Eq. (11) and the corresponding wave functions have the period 4π in φ, rather than conventional 2π. Although at $\varphi = 2\pi$ the spectrum in the left panel of Fig. 1,*c* is the same as at $\varphi = 0$, the occupation numbers are different. The lower state is empty and the upper state is occupied. Only at $\varphi = 4\pi$ the occupation numbers are the same as at $\varphi = 0$.

The 4π periodicity is the consequence of the energy levels crossing at $\varphi = \pi$. In contrast, in the *s*-wave case, the levels repel at $\varphi = \pi$ in Fig. 1,*b*, thus the energy curves are 2π-periodic. As discussed at the end of Sec. 4.1, there is no matrix element between the crossing energy levels at $\varphi = \pi$. Thus, there are no transitions between them, so the occupation numbers of the solid and dotted curves in Fig. 1,*c* are preserved. In order to show this more formally, we can write a general solution of the time-dependent BdG equation as a superposition of the two subgap states with the time-dependent $\varphi(t)$: $\psi(t) = \sum_a C_a(t)\psi_a[\varphi(t)]$. The matrix element of transitions between the states is proportional to $\dot{\varphi}\langle\psi_+|\partial_\varphi\psi_-\rangle = \dot{\varphi}\langle\psi_+|\partial_\varphi\hat{H}|\psi_-\rangle/(E_- - E_+)$. We found that it is zero in the p_x-wave case, thus there are no transitions, and the initial occupation numbers of the subgap states at $\varphi = 0$ are preserved dynamically.

As one can see in Fig. 1,*c*, the system is not in the ground state when $\pi < \varphi < 3\pi$, because the upper energy level is occupied and the lower one is empty. In principle, the system might be able to relax to the ground state by emitting a phonon or a photon. At present time, we do not have an explicit estimate for such inelastic relaxation time, but we expect that it is quite long. (The other papers [18,19,21,22] that assume thermodynamic equilibrium for each value of the phase φ do not have an estimate of the relaxation time either.) To observe the predicted ac Josephson effect with the fractional frequency $eV/\hbar$, the period of Josephson oscillations should be set shorter than the inelastic relaxation time, but not too short, so that the time evolution of the BdG equation can be treated adiabatically. Controlled nonequilibrium population of the upper Andreev bound state was recently achieved experimentally in a *s*-wave Josephson junction in Ref. 32.

Equation (17) can be generalized to the case where initially the two subgap states are populated thermally at $\varphi = 0$, and these occupation numbers are preserved by dynamical evolution

$$I_p(t) = \frac{2e}{\hbar}\sum_a \frac{\partial E_a[\varphi(t)]}{\partial\varphi} f[E_a(\varphi = 0)] = \quad (18)$$

$$= \sin\left(\frac{eVt}{\hbar}\right)\frac{\pi\Delta_0}{\sqrt{D}eR}\tanh\left(\frac{\Delta_0\sqrt{D}}{2T}\right). \quad (19)$$

Note that the periodicities of the dynamical equation (16) and the thermodynamic Eq. (19) are different. The latter equation assumes that the occupation numbers of the subgap states are in instantaneous thermal equilibrium for each φ.

4.4. Tunneling Hamiltonian approach

In the infinite barrier limit $D \to 0$, the energies $\pm E_0^{(p)}$ of the two subgap states (11) degenerate to zero, i.e., they become midgap states. The wave functions (8) are simplified as follows:

$$\psi_{\pm 0} = \frac{\psi_{L0}(x) \mp \psi_{R0}(x)}{\sqrt{2}}, \quad (20)$$

$$\psi_{L0} = \sqrt{2\kappa}\sin(k_F x)\, e^{\kappa x}\begin{pmatrix}1\\ i\end{pmatrix}\theta(-x), \qquad (21)$$

$$\psi_{R0} = \sqrt{2\kappa}\sin(k_F x)\, e^{-\kappa x}\begin{pmatrix}e^{i\varphi/2}\\ -ie^{-i\varphi/2}\end{pmatrix}\theta(x). \qquad (22)$$

Since at $D = 0$ the Josephson junction consists of two semi-infinite uncoupled p_x-wave superconductors, ψ_{L0} and ψ_{R0} are the wave functions of the surface midgap states [15] belonging to the left and right superconductors. Let us examine the properties of the midgap states in more detail.

If (u,v) is an eigenvector of Eq. (3) with an eigenvalue E_n, then $(-v^*,u^*)$ for s-wave and (v^*,u^*) for p-wave are the eigenvectors with the energy $E_{\bar{n}} = -E_n$. It follows from these relations and Eq. (1) that $\hat{\gamma}_{\bar{n}\bar{\sigma}\bar{k}_y} = C\hat{\gamma}^\dagger_{n\sigma k_y}$ with $|C| = 1$. Notice that in the s-wave case, because (u,v) and $(-v^*,u^*)$ are orthogonal for any u and v, the states n and $\bar{n}$ are always different. However, in the p-wave case, the vectors (u,v) and (v^*,u^*) may be proportional, in which case they describe the same state with $E = 0$. The states (21) and (22) indeed have this property:

$$v_{L0} = iu^*_{L0}, \qquad v_{R0} = -iu^*_{R0}. \qquad (23)$$

Substituting Eq. (23) into Eq. (1), we find the Bogoliubov operators of the left and right midgap states

$$\hat{\gamma}^\dagger_{L0\sigma k_y} = i\hat{\gamma}_{L0\bar{\sigma}\bar{k}_y}, \quad \hat{\gamma}^\dagger_{R0\sigma k_y} = -i\hat{\gamma}_{R0\bar{\sigma}\bar{k}_y}. \qquad (24)$$

Operators (24) correspond to the Majorana fermions discussed in Ref. 24. In the presence of a midgap state, the sum over n in Eq. (2) should be understood as $\sum_{n>0} + 1/2\sum_{n=0}$, where we identify the second term as the projection $\mathcal{P}\hat{c}$ of the electron operator onto the midgap state. Using Eqs. (23), (24), and (2), we find

$$\mathcal{P}\hat{c}_{\sigma k_y}(x) = u_0(x)\hat{\gamma}_{0\sigma k_y} = v_0^*(x)\hat{\gamma}^\dagger_{0\bar{\sigma}\bar{k}_y}. \qquad (25)$$

Let us consider two semi-infinite p_x-wave superconductors on a 1D lattice with the spacing l, one occupying $x \le \bar{l} = -l$ and another $x \ge l$. They are coupled by the tunneling matrix element τ between the sites $\bar{l}$ and l:

$$\hat{H}_\tau = \tau\sum_{\sigma k_y}[\hat{c}^\dagger_{L\sigma k_y}(\bar{l})\hat{c}_{R\sigma k_y}(l) + \hat{c}^\dagger_{R\sigma k_y}(l)\,\hat{c}_{L\sigma k_y}(\bar{l})]. \qquad (26)$$

In the absence of coupling ($\tau = 0$), the subgap wave functions of each superconductor are given by Eqs. (21) and (22). Using Eqs. (25), (23), (21), and (22), the tunneling Hamiltonian projected onto the basis of midgap states is

$$\mathcal{P}\hat{H}_\tau = \tau\,[u^*_{L0}(\bar{l})u_{R0}(l) + \text{c.c.}](\hat{\gamma}^\dagger_{L0\uparrow}\hat{\gamma}_{R0\uparrow} + \text{H.c.}) =$$

$$= \Delta_0\sqrt{D}\cos(\varphi/2)(\hat{\gamma}^\dagger_{L0\uparrow}\hat{\gamma}_{R0\uparrow} + \hat{\gamma}^\dagger_{R0\uparrow}\hat{\gamma}_{L0\uparrow}), \qquad (27)$$

where $\sqrt{D} = 4\tau\sin^2 k_F l/\hbar v_F$ is the transmission amplitude, and we omitted summation over the diagonal index k_y. Notice that Eq. (27) is 4π-periodic in φ [24].

Hamiltonian (27) operates between the two degenerate states of the system related by annihilation of the Bogoliubov quasiparticle in the right midgap state and its creation in the left midgap state. In this basis, Hamiltonian (27) can be written as a 2×2 matrix

$$\mathcal{P}\hat{H}_\tau = \Delta_0\sqrt{D}\cos(\varphi/2)\begin{pmatrix}0 & 1\\ 1 & 0\end{pmatrix}. \qquad (28)$$

The eigenvectors of Hamiltonian (28) are $(1, \mp 1)$, i.e., the antisymmetric and symmetric combinations of the right and left midgap states given in Eq. (20). Their eigenenergies are $E_\pm(\varphi) = \mp\Delta_0\sqrt{D}\cos(\varphi/2)$, in agreement with Eq. (11). The tunneling current operator is obtained by differentiating Eqs. (27) or (28) with respect to φ. Because φ appears only in the prefactor, the operator structures of the current operator and the Hamiltonian are the same, so they are diagonal in the same basis. Thus, the energy eigenstates are simultaneously the eigenstates of the current operator with the eigenvalues

$$I_\pm = \pm\sqrt{D}e\frac{\Delta_0}{\hbar}\sin\left(\frac{\varphi}{2}\right), \qquad (29)$$

in agreement with Eq. (17). The same basis $(1, \mp 1)$ diagonalizes Hamiltonian (28) even when a voltage V is applied and the phase φ is time-dependent. Then the initially populated eigenstate with the lower energy produces the current $I_p = \sqrt{D}(e\Delta_0/\hbar)\sin(eVt/\hbar)$ with the fractional Josephson frequency $eV/\hbar$, in agreement with Eq. (17).

4.5. Josephson current carried by single electrons, rather than Cooper pairs

In the tunneling limit, the transmission coefficient D is proportional to the square of the electron tunneling amplitude τ: $D \propto \tau^2$. Eqs. (17) and (29) show that the Josephson current in the p_x-p_x junction is proportional to the first power of the electron tunneling amplitude τ. This is in contrast to the $s-s$ junction, where the Josephson current (14) is proportional to τ^2. This difference results in the big ratio $I_p/I_s = 2/\sqrt{D}$ between the critical currents at $T = 0$ in

the p_x- and s-wave cases, as shown in Fig. 2 and discussed in Sec. 4.2. The reason for the different powers of τ is the following. In the p_x-wave case, the transfer of just one electron between the degenerate left and right midgap states is a real (nonvirtual) process. Thus, the eigenenergies are determined from the secular equation (28) already in the first order of τ. In the s-wave case, there are no midgap states, so the transferred electron is taken from below the gap and placed above the gap, at the energy $\cosh 2\Delta_0$. Thus, the transfer of a single electron is a virtual (not real) process. It must be followed by the transfer of another electron, so that the pair of electrons is absorbed into the condensate. This gives the current proportional to τ^2.

This picture implies that the Josephson supercurrent across the interface is carried by single electrons in the p_x-p_x junction and by Cooper pairs in the $s-s$ junction. Because the single-electron charge e is a half of the Cooper-pair charge $2e$, the frequency of the ac Josephson effect in the p_x-p_x junction is $eV/\hbar$, a half of the conventional Josephson frequency $2eV/\hbar$ for the $s-s$ junction. These conclusions also apply to a junction between two cuprate d-wave superconductors in such orientation that both sides of the junction have surface midgap states, e.g., to the 45°/45° junction (see Sec. 5).

In both the p_x-p_x and $s-s$ junctions, electrons transferred across the interface are taken away into the bulk by the supercurrent of Cooper pairs. In the case of the p_x-p_x junction, a single transferred electron occupies a midgap state until another electron gets transferred. Then the pair of electrons becomes absorbed into the bulk condensate, the midgap state returns to the original configuration, and the cycle repeats. In the case of the $s-s$ junction, two electrons are simultaneously transferred across the interface and become absorbed into the condensate. Clearly, electric charge is transferred across the interface by single electrons at the rate proportional to τ in the first case and by Cooper pairs at the rate proportional to τ^2 in the second case, but the bulk supercurrent is carried by the Cooper pairs in both cases.

5. Josephson junctions between *d*-wave superconductors

In this section, we study Josephson junctions between two d-wave cuprate superconductors. As before, we select the coordinate x perpendicular to the junction line and assume that the electron momentum component k_y parallel to the junction line is a conserved good quantum number. Then, the 2D problem separates into a set of 1D solutions (8) in the x direction labeled by the index k_y. Using an isotropic electron energy dispersion law $\varepsilon = \hbar^2(k_x^2 + k_y^2)/2m - \mu$, we replace the Fermi momentum k_F and velocity v_F by their x-components $k_{Fx} = \sqrt{k_F^2 - k_y^2}$ and $v_{Fx} = \hbar k_{Fx}/m$. Thus, the transmission coefficient D in Eq. (7) becomes k_y-dependent. The total Josephson current is given by a sum over all occupied subgap states labeled by k_y.

For the cuprates, let us consider a junction parallel to the $[1,\bar{1}]$ crystal direction in the $a-b$ plane and select the x axis along the diagonal [1,1], as shown in Fig. 3,*a*. In these coordinates, the d-wave pairing potential is

$$\hat{\Delta}_{\sigma k_y}(x,\hat{k}_x) = \sigma 2\Delta_\beta k_y \hat{k}_x / k_F^2, \qquad (30)$$

where the same notation as in Eq. (4) is used. Direct comparison of Eqs. (30) and (4) demonstrates that the d-wave superconductor with the 45° junction maps to the p_x-wave superconductor by the substitution $\Delta_0 \to \sigma 2\Delta_0 k_y/k_F$. Thus, the results obtained in Sec. 4 for the p_x-p_x junction apply to the 45°/45° junction between two d-wave superconductors with the appropriate integration over k_y. The energies and the wave functions of the subgap Andreev states in the 45°/45° junction are 4π-periodic, as in Eqs. (11). Thus the ac Josephson current has the fractional frequency $eV/\hbar$, as in Eq. (17).

On the other hand, if the junction is parallel to the [0,1] crystal direction, as shown in Fig. 3,*b*, then $\hat{\Delta}_{\sigma k_y}(x,\hat{k}_x) = \sigma\Delta_\beta(\hat{k}_x^2 - k_y^2)/k_F^2$. This pairing potential is an even function of k_x, thus it is analogous to the s-wave pairing potential in Eq. (4). Thus, the 0°/0° junction between two d-wave superconductors is analogous to the $s-s$ junction. It should exhibit the conventional 2π-periodic Josephson effect with the frequency $2eV/\hbar$.

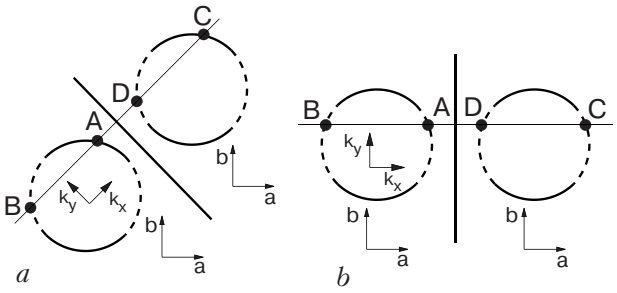

Fig. 3. Schematic drawing of the 45°/45° junction (*a*) and 0°/0° junction (*b*) between two d-wave superconductors. The thick line represents the junction line. The circles illustrate the Fermi surfaces, where positive and negative pairing potentials Δ are shown by the solid and dotted lines. The points A, B, C, and D in the momentum space are connected by transmission and reflection from the barrier.

For a generic orientation of the junction line, the d-wave pairing potential acts like p_x-wave for some momenta k_y and like s-wave for other k_y. Thus, the total Josephson current is a sum of the unconventional and conventional terms [20]:

$$I = C_1 \sin(\varphi/2) + C_2 \sin(\varphi) + \ldots, \qquad (31)$$

with some coefficients C_1 and C_2. We expect that both terms in Eq. (31) are present for any real junction between d-wave superconductors because of imperfections. However, the ratio C_1/C_2 should be maximal for the junction shown in Fig. 3,*a* and minimal for the junction shown in Fig. 3,*b*.

6. Experimental observation of the fractional ac Josephson effect

Conceptually, the setup for experimental observation of the fractional ac Josephson effect is straightforward. One should apply a dc voltage V to the junction and measure frequency spectrum of microwave radiation from the junction, expecting to detect a peak at the fractional frequency $eV/\hbar$. To observe the fractional ac Josephson effect predicted in this paper, it is necessary to perform this experiment with the 45°/45° cuprate junctions shown in Fig. 3,*a*. For control purposes, it is also desirable to measure frequency spectrum for the 0°/0° junction shown in Fig. 3,*b*, where a peak at the frequency $eV/\hbar$ should be minimal. It should be absent completely in a conventional $s-s$ junction, unless the junction enters a chaotic regime with period doubling [33]. The high-T_c junctions of the required geometry can be manufactured using the step-edge technique. Bicrystal junctions are not appropriate, because the crystal axes **a** and **b** of the two superconductors are rotated relative to each other in such junctions. As shown in Fig. 3,*a*, we need the junction where the crystal axes of the two superconductors have the same orientation. Unfortunately, attempts to manufacture Josephson junctions from the Q1D organic superconductors $(TMTSF)_2X$ failed thus far.

The most common way of studying the ac Josephson effect is observation of the Shapiro steps [34]. In this setup, the Josephson junction is irradiated by microwaves with the frequency ω, and steps in dc current are detected at the dc voltages $V_n = n\hbar\omega/2e$. Unfortunately, this method is not very useful to study the effect that we predict. Indeed, our results are effectively obtained by the substitution $2e \to e$. Thus, we expect to see the Shapiro steps at the voltages $V_m = m\hbar\omega/e = 2m\hbar\omega/2e$, i.e., we expect to see only even Shapiro steps. However, when both terms are present in Eq. (31), they produce both even and odd Shapiro steps, so it would be difficult to differentiate the novel effect from the conventional Shapiro effect. Notice also that the so-called fractional Shapiro steps observed at the voltage $V_{1/2} = \hbar\omega/4e$ corresponding to $n = 1/2$ have nothing to do with the effect that we propose. They originate from the higher harmonics in the current-phase relation $I \propto \sin(2\varphi)$. The fractional Shapiro steps have been observed in cuprates [35], but also in conventional s-wave superconductors [36]. Another method of measuring the current-phase relation in cuprates was employed in Ref. 37, but connection with our theoretical results is not clear at the moment.

7. Conclusions

In this paper, we study suitably oriented p_x-p_x or $d-d$ Josephson junctions, where the superconductors on both sides of the junction originally have the surface Andreev midgap states. In such junctions, the Josephson current I, carried by the hybridized subgap Andreev bound states, is a 4π-periodic function of the phase difference φ: $I \propto \sin(\varphi/2)$, in agreement with Ref. 24. Thus, the ac Josephson current should exhibit the fractional frequency $eV/\hbar$, a half of the conventional Josephson frequency $2eV/\hbar$. In the tunneling limit, the Josephson current is proportional to the first power of the electron tunneling amplitude, not the square as in the conventional case [21–23]. Thus, the Josephson current in the considered case is carried by single electrons with charge e, rather than by Copper pairs with charge $2e$. The fractional ac Josephson effect can be observed experimentally by measuring frequency spectrum of microwave radiation from the junction and detecting a peak at $eV/\hbar$.

The work was supported by NSF Grant DMR-0137726. K. Sengupta thanks S.M. Girvin for support.

1. B.D. Josephson, *Phys. Lett.* **1**, 251 (1962).
2. I.K. Yanson, V.M. Svistunov, and I.M. Dmitrenko, *Sov. Phys. JETP* **21**, 650 (1965).
3. I.M. Dmitrenko and I.K. Yanson, *JETP Lett.* **2**, 154 (1965).
4. D.N. Langenberg, D.J. Scalapino, B.N. Taylor, and R.E. Eck, *Phys. Rev. Lett.* **15**, 294 (1965).
5. I.M. Dmitrenko, I.K. Yanson, and I.I. Yurchenko, *Sov. Phys. Solid State* **9**, 2889 (1968).
6. I.O. Kulik and I.K. Yanson, *The Josephson Effect in Superconducting Tunneling Structures, Israel Program for Scientific Translations,* Jerusalem (1972).
7. A.K. Jain, K.K. Likharev, J.E. Lukens, and J.E. Savageau, *Phys. Rept.* **109**, 309 (1984).
8. R. Kleiner, F. Steinmeyer, G. Kunkel, and P. Müller, *Phys. Rev. Lett.* **68**, 2394 (1992).
9. D.J. Van Harlingen, *Rev. Mod. Phys.* **67**, 515 (1995); C. Tsuei and J. Kirtley, *ibid.* **72**, 969 (2000).

10. TMTSF stands for tetramethyltetraselenafulvalene, and X represents inorganic anions such as ClO_4 or PF_6.
11. I.J. Lee et al., *Phys. Rev. Lett*. **88**, 017004 (2002); I.J. Lee, M.J. Naughton, G.M. Danner, and P.M. Chaikin, *ibid*. **78**, 3555 (1997); I.J. Lee, P.M. Chaikin, and M.J. Naughton, *Phys. Rev.* **B62**, R14669 (2000).
12. A.G. Lebed, *Phys. Rev.* **B59**, R721 (1999); A.G. Lebed, K. Machida, and M. Ozaki, *ibid*. **62**, R795 (2000).
13. C.-R. Hu, *Phys. Rev. Lett*. **72**, 1526 (1994).
14. S. Kashiwaya and Y. Tanaka, *Rep. Prog. Phys*. **63**, 1641 (2000).
15. K. Sengupta, I. Zutić, H.-J. Kwon, V.M. Yakovenko, and S. Das Sarma, *Phys. Rev.* **B63**, 144531 (2001).
16. Y. Tanuma, K. Kuroki, Y. Tanaka, and S. Kashiwaya, *Phys. Rev.* **B64**, 214510 (2001); Y. Tanuma et al., **66**, 094507 (2002).
17. T. Löfwander, V.S. Shumeiko, and G. Wendin, *Supercond. Sci. Technol.* **14**, R53 (2001).
18. Y. Tanaka, T. Hirai, K. Kusakabe, and S. Kashiwaya, *Phys. Rev.* **B60**, 6308 (1999).
19. C.D. Vaccarella, R.D. Duncan, and C.A.R. Sá de Melo, *Physica* **C391**, 89 (2003).
20. The current-phase relation $I \propto \sin(\varphi/2)$ that we propose should not be confused with another unconventional current-phase relation $I \propto \sin(2\varphi)$ with the period π, which was predicted theoretically for junctions between *s*- and *d*-wave superconductors [38,39], *s*- and *p*-wave superconductors [38,40], and for the $0^\circ/45^\circ$ junctions between two *d*-wave superconductors [41].
21. Y. Tanaka and S. Kashiwaya, *Phys. Rev.* **B56**, 892 (1997).
22. R.A. Riedel and P.F. Bagwell, *Phys. Rev.* **B57**, 6084 (1998).
23. Yu.S. Barash, *Phys. Rev*. **B61**, 678 (2000).
24. A.Yu. Kitaev, *cond-mat/*0010440.
25. A.M. Zagoskin, *Quantum Theory of Many-Body Systems,* Springer, New York (1998).
26. A. Furusaki, *Superlattices Microstruct*. **25**, 809 (1999).
27. Y. Tanaka and S. Kashiwaya, *Phys. Rev.* **B53**, 9371 (1996).
28. Eq. (12) can be equivalently obtained as a difference between the right- and left-moving currents using the formula $I_a = ev_F(|A_a|^2 - |B_a|^2)$ with the normalization condition $\int dx|\psi^2| = 1$ [26].
29. V. Ambegaokar and A. Baratoff, *Phys. Rev. Lett*. **10**, 486 (1963); *ibid*. **11**, 104 (1963).
30. I.O. Kulik and A.N. Omel'yanchuk, *Fiz. Nizk. Temp*. **4**, 296 (1978) [*Sov. J. Low Temp. Phys*. **4**, 142 (1978)].
31. H. Arie, K. Yasuda, H. Kobayashi, I. Iguchi, Y. Tanaka, and S. Kashiwaya, *Phys. Rev.* **B62**, 11864 (2000).
32. J.J.A. Baselmans, T.T. Heikkilä, B.J. van Wees, and T.M. Klapwijk, *Phys. Rev. Lett*. **89**, 207002 (2002).
33. R.F. Miracky, J. Clarke, and R.H. Koch, *Phys. Rev. Lett*. **50**, 856 (1983); C.B. Whan, C.J. Lobb, and M.G. Forrester, *J. Appl. Phys*. **77**, 382 (1995).
34. S. Shapiro, *Phys. Rev. Lett*. **11**, 80 (1963); S. Shapiro, A.R. Janus, and S. Holly, *Rev. Mod. Phys*. **36**, 223 (1964).
35. E.A. Early, A.F. Clark, and K. Char, *Appl. Phys. Lett.* **62**, 3357 (1993); L.C. Ku et al., *Physica* **C229**, 320 (1994); I.V. Borisenko et al., *Physica* **C368**, 328 (2002).
36. J. Clarke, *Phys. Rev. Lett*. **21**, 1566 (1968).
37. E. Il'ichev et al., *Phys. Rev. Lett*. **86**, 5369 (2001).
38. S. Yip, *J. Low Temp. Phys*. **91**, 203 (1993).
39. Y. Tanaka, *Phys. Rev. Lett*. **72**, 3871 (1994); A.M. Zagoskin, *J. Phys. Condens. Matter* **9**, L419 (1997).
40. N. Yoshida, Y. Tanaka, S. Kashiwaya, and J. Inoue, *J. Low Temp. Phys*. **117**, 563 (1999).
41. T. Löfwander, G. Johansson, M. Hurd, and G. Wendin, *Phys. Rev.* **B57**, R3225 (1998); M. Hurd, T. Löfwander, G. Johansson, and G. Wendin, *ibid*. **59**, 4412 (1999).